Wearable Technologies (2026), 7, e12
doi:10.1017/wtc.2026.10047

CAMBRIDGE UNIVERSITY PRESS

Wearable-only estimation of L5-S1 joint moments during lifting: A CEINMS-based validation

Filippo Motta[1,2], Mohamed Irfan Refai[3], Alberto Ranavolo[2], Tiwana Varrecchia[2], Massimo Sartori[3] and Manuela Galli[1]

[1]Dipartimento di Elettronica, Informazione e Bioingegneria, Politecnico di Milano, Italy
[2]INAIL, Italy
[3]Faculty of Engineering Technology, University of Twente, Netherlands
Corresponding author: Mohamed Irfan Refai; Email: m.i.mohamedrefai@utwente.nl

Received: 23 December 2025 UTC; **Revised:** 18 March 2026 UTC; **Accepted:** 27 June 2026 UTC

Keywords: biomechanics; industry; sensors

Abstract

This study aimed to evaluate the use of wearable sensors to estimate L5-S1 flexion moments during symmetric lifting tasks by integrating inertial motion capture (IMC), surface electromyography (sEMG), and the calibrated EMG-informed neuromusculoskeletal (CEINMS) framework. Eight participants performed stoop and squat lifting at four load levels while gold-standard optoelectronic motion capture, ground reaction forces, inertial measurement units (IMUs), and sEMG were recorded. IMC-based inverse dynamics showed excellent agreement with OMC (ρ = 0.83–0.96; ICC > 0.91), with mean errors around 2–3 Nm. CEINMS moments calibrated using wearable data exhibited strong reliability and captured the expected load-dependent increases in lumbar moments, although peak values during heavy lifting were systematically underestimated. IMC consistently underestimated L5-S1 flexion angles by 2°, likely contributing to the reduced peak moment estimates. Overall, findings support the feasibility of a wearables-only approach for ergonomic risk assessment. Future work should focus on improving lumbo-sacral flexion angle estimation from IMUs, potentially through multi-sensor lumbar configurations.

1. Introduction

Low back disorders, frequently triggered by repetitive lifting tasks and elevated mechanical loading of the lumbar spine, remain among the most prevalent work-related musculoskeletal injuries (Coenen et al., 2014; Jahn et al., 2023). Excessive flexion-extension angle, moments, and compression forces at the L5-S1 joint are recognized as critical risk factors for the development of chronic low back pain (Murtezani et al., 2011; Coenen et al., 2013). To better understand these mechanisms, musculoskeletal modeling has become an indispensable tool for estimating internal joint loading and muscle forces, thereby providing a bridge between external motion, force measurements, and spinal kinetics (Abdullah et al., 2024). Such models are central for monitoring biomechanical exposure and informing preventive strategies in occupational ergonomics, rehabilitation, and assistive system design.

A variety of modeling approaches exist. Some rely purely on kinematic and kinetic data obtained from laboratory equipment, while others employ inverse dynamics coupled with static optimization to estimate

M.S. and M.G. shared last authorship.

© The Author(s), 2026. Published by Cambridge University Press. This is an Open Access article, distributed under the terms of the Creative Commons Attribution licence (http://creativecommons.org/licenses/by/4.0), which permits unrestricted re-use, distribution and reproduction, provided the original article is properly cited.

Downloaded from https://www.cambridge.org/core. 19 Nov 2026 at 05:43:20, subject to the Cambridge Core terms of use.

joint moments and muscle forces (e.g., using the OpenSim framework; Delp et al., 2007). Musculoskeletal modeling, often within multi-body dynamics, is used to represent rigid segments, joint kinematics, and musculotendon actuators for predicting internal loads during complex tasks (such as gait or sit-to-stand maneuvers) (Abdullah et al., 2024). Finite element (FE) musculoskeletal models account for three-dimensional muscle geometry, enabling predictions of muscle contractions and mechanical interactions beyond simple line-segment representations (Li et al., 2019; Galbusera et al., 2020). Unlike traditional multi-body models, which treat body segments as rigid links connected by idealized joints, FE-based approaches can simulate the deformation of bones, intervertebral discs, and soft tissues under load. This allows for a more detailed assessment of local stress and strain distributions within muscles and spinal structures, providing insights into the mechanical pathways that lead to tissue overload and injury. Such models are particularly useful for studying the internal mechanics of the lumbar spine, as they can account for complex geometries and material heterogeneity of vertebral and disc tissues (Galbusera et al., 2020). However, despite their accuracy, FE musculoskeletal models require subject-specific imaging data and high computational resources, limiting their use in dynamic or real-time applications.

Several neuromusculoskeletal modeling approaches integrate EMG-derived muscle activations to estimate muscle forces or joint moments, including the classical EMG-driven models proposed by Buchanan and Lloyd (Lloyd and Besier, 2003; Buchanan et al., 2004), hybrid EMG-assisted inverse dynamics frameworks (Shakourisalim et al., 2024). In this context, the calibrated EMG-informed neuromusculoskeletal (CEINMS) framework enables the estimation of joint moments through the integration of kinematic inputs with muscle activation data (Pizzolato et al., 2015). CEINMS has been successfully applied in controlled settings, including lifting tasks, but its implementations have so far remained largely confined to laboratory environments where gold-standard motion capture and force plates are available (Moya-Esteban et al., 2022; Feola et al., 2023). The same limitation applies to most modeling techniques, whether inverse dynamics or EMG-assisted. This dependence severely limits their applicability in real workplaces, where most hazardous lifting occurs. Occupational risk assessment requires monitoring tools capable of estimating internal spinal loading outside controlled environments.

Recent advances in wearable technologies suggest that the input data required by the CEINMS framework, namely muscle activations and kinematics, can be acquired through wearable sensors, potentially enabling its application outside the lab (Ghamkhar and Kahlaee, 2015; Papi et al., 2017). Surface EMG has long been employed to reveal muscle activation patterns relevant to spinal loading (Geisser et al., 2005; Lathlean et al., 2024), and new approaches, such as inverse synergy methods (Rook et al., 2025), highlight the potential to refine EMG-informed models even further.

Static optimization and redundancy-resolution methods used in classical inverse dynamics rely on minimizing a cost function, commonly a function of muscle activation or stress, to predict how muscles share the load around a joint. However, the validity of these assumptions is debated, as the "optimality" criteria may not generalize across different movement types, fatigue states, injury levels, or lifting strategies (Crowninshield and Brand, 1981). EMG-driven models overcome these limitations by using recorded muscle activations, thereby incorporating the subject's true neuromuscular strategy rather than relying on assumed coordination patterns. This makes EMG-driven modeling particularly important for lifting, where co-contraction, fatigue, and task-specific strategies heavily influence spinal loading.

Wearable inertial motion capture (IMC) systems have emerged as a promising alternative to opto-electronic motion capture (OMC), offering the ability to capture whole-body and trunk kinematics in naturalistic conditions (Palmieri et al., 2023; Motta et al., 2024; Varrecchia et al., 2024; Motta et al., 2025). Several studies have validated IMC against OMC, both for full-body and trunk-level kinematics (Dal Farra et al., 2025; Villa et al., 2025), and more specifically, IMC-based methods have been proposed for estimating L5-S1 joint kinetics (Muller et al., 2022; Nail-Ulloa et al., 2024).

Hence, although studies have evaluated the use of surface electromyography (sEMG) to measure spine muscle activation and IMC for lifting kinematics, a gap remains in utilizing and validating these two systems against OMC as a source of data for CEINMS to analyze lifting tasks and back load. Bridging this gap could enable the development of a practical tool for assessing workers' ergonomic risk during lifting tasks through direct measurement and estimation of key biomechanical variables, such as joint angles and

Downloaded from https://www.cambridge.org/core. 19 Nov 2026 at 05:43:20, subject to the Cambridge Core terms of use.

moments. Thus, the claim of a "wearable-only model" is novel not in the use of these sensors, but in demonstrating that both the kinematic and the neuromuscular components required by a framework like CEINMS can be derived exclusively from wearable data. This represents a step toward practical on-site risk assessment tools.

This study aims to evaluate if a wearable-only system can be used to estimate L5-S1 flexion moment during a lifting task. The actions carried out for this purpose are: (i) evaluate the estimation of flexion-extension angles at the L5-S1 joint during symmetric lifting tasks using IMC compared to OMC, and (ii) integrate the kinetics from IMC with sEMG data in CEINMS to validate the L5-S1 moment estimates obtained by a wearables-only approach. A systematic comparison will help determine whether CEINMS can be exploited using IMC kinetics and if a wearable-only system can be reliable in joint moment estimation to support ergonomic risk assessment outside laboratory settings.

2. Materials and methods

2.1. Experimental protocol

The study was approved by the Ethical Committee of the University of Twente (ref. 240909). Eight healthy adults (four males, four females; 24 ± 2.5 years; 74.9 ± 11.4 kg; 180 ± 6.4 cm) participated after providing written informed consent. Six bipolar surface EMG electrodes (Cometa, Italy; 2,000 Hz) were placed bilaterally on three back muscles (Longissimus thoracis pars lumborum, Longissimus thoracis pars thoracis, and Iliocostalis), as shown in Figure 1. These muscles were selected because previous literature demonstrated that they are the primary superficial lumbar extensors contributing to L5-S1 flexion-extension moment generation and can be reliably measured using surface EMG (Varrecchia et al., 2022; Mohamed Refai et al., 2024). Deep muscles such as multifidus were not included due to the limitations of non-invasive EMG acquisition. Maximum voluntary contractions (MVCs) were recorded for normalization. Participants were positioned in a prone position on a treatment table and instructed to perform a maximal isometric trunk extension while an operator applied manual resistance against the upper trunk to oppose the movement. Each MVC lasted approximately 5 s and was repeated three times, with the highest EMG amplitude retained for normalization, following procedures commonly adopted in trunk EMG studies (Vera-Garcia et al., 2010). Sixty-six retroreflective markers were used, 62 on each participant (modified Cleveland Clinic marker set) (Elliott et al., 2013) and four attached to the corners of

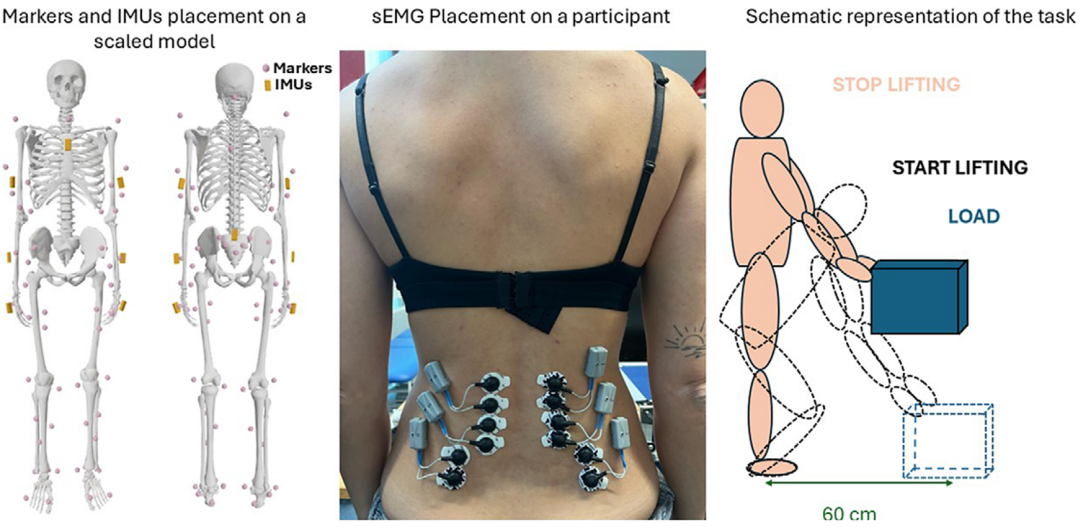


Figure 1. *Markers (pink spheres) and IMUs (orange boxes) placement presented on a scaled model (left), sEMG placement on a participant (center), and schematic representation of the task (right).*

Downloaded from https://www.cambridge.org/core. 19 Nov 2026 at 05:43:20, subject to the Cambridge Core terms of use.

the external load (box), acquired at 100 Hz by a 12-camera optical motion capture system (Qualisys, Medical AB, Sweden). In addition, eight inertial measurement units (IMUs; Xsens, Movella, US; 60 Hz) were placed on the upper body according to the manufacturer's guidelines (Roetenberg et al., 2009). Both markers and IMUs placement are shown in Figure 1.

Ground reaction forces (GRFs) were recorded using a force platform (AMTI, MA; 2,048 Hz). Following IMC calibration, participants performed a static trial and two lifting tasks: stooping (knees extended) and squatting (knees flexed). For each task, four loads (0, 5, 10, and 15 kg) were lifted ten times within 2 min, guided by a metronome. The order of loads and tasks was randomized across participants. Participants lifted the box from the floor to an upright standing posture while holding the load close to the body. The movement ended once the participant reached a fully upright position, resulting in the load being approximately at hip level. The initial box position was standardized on the floor directly in front of the participant's feet, at a distance of 60 cm, to ensure consistency across trials.

2.2. Data processing

The overall workflow of data processing is summarized in Figure 2. As the first step, marker trajectories were labeled and then processed in OpenSim (OS). For each subject, the Lifting Full Body (LFB) Model was scaled to the static trial. This model was selected because it was specifically developed and validated for the biomechanical analysis of lifting tasks, adding a detailed representation of trunk muscles and lumbar spine mechanics. This makes it particularly suitable for estimating lumbar joint moments during manual material handling (Beaucage-Gauvreau et al., 2019). From the OMC data, the joint angles were estimated using the OS's inverse kinematics tool.

For IMC data, IMU locations were determined using the OS IMU Placer tool, which positions virtual sensors on the musculoskeletal model. The tool aligns each sensor with the corresponding body segment by applying a fixed rotation, represented as a direction cosine matrix, that transforms the IMU local reference frame into the segment reference frame. This transformation is defined as

$$R_{\text{segment}} = R_{\text{sensor}} \cdot R_{\text{offset}},$$

where R_{sensor} is the orientation of the IMU in the global frame, and R_{offset} is the calibration rotation obtained during the static trial, representing the orientation of the sensor with respect to the anatomical segment.

The IMU inverse kinematics tool was then used to compute joint angles by minimizing the difference between measured IMU orientations and the orientations of the corresponding body segments in the musculoskeletal model (Al Borno et al., 2022).

It is important to note that the definition of the L5-S1 joint angle differs between OMC- and IMC-based modeling pipelines. In OMC, the angle is derived from relative marker-based segment orientations within the scaled musculoskeletal model, while in IMC, it is reconstructed from virtual sensor orientations

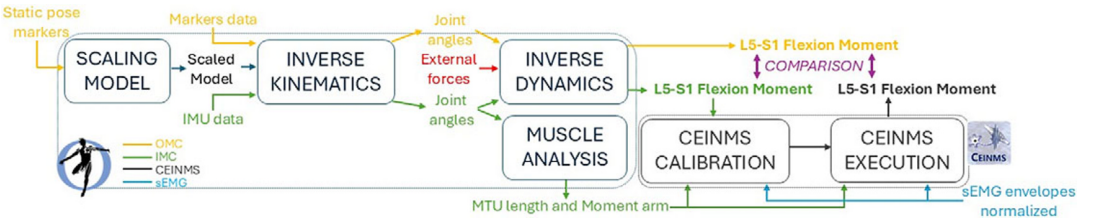


Figure 2. *Data processing workflow. The lines indicate the data processing: in yellow the OMC, in green the IMC, in grey the CEINMS, and in light blue the surface electromyography (sEMG).*

Downloaded from https://www.cambridge.org/core. 19 Nov 2026 at 05:43:20, subject to the Cambridge Core terms of use.

constrained to the corresponding body segments. As a result, the estimated ranges of flexion-extension differ between methods, even for the same movement.

Muscle-tendon lengths and moment arms were obtained via the Muscle Analysis tool, while the flexion moment at the L5-S1 joint was calculated using the Inverse Dynamics tool. Inputs for inverse dynamics included subject kinematics (marker- or IMU-based), box kinematics, and external loads. EMG signals were processed in MATLAB to extract linear envelopes, which were normalized using MVC values.

CEINMS calibration used joint angles (from IMC data), muscle-tendon lengths, moment arms, muscle activations, and IMC-derived joint moments as reference. The musculoskeletal model includes a large set of back muscles modelled by 190 muscle-tendon units (MTUs). EMG signals were recorded only from six muscles, covering 126 MTUs in the model. For the muscles without EMG measurement, only the passive contributions were considered as presented in previous works (Moya-Esteban et al., 2022; Mohamed Refai et al., 2024). To test the ability of the model to generalize across loading conditions, the CEINMS model calibration was performed using only the 0 and 15 kg trials. Once calibrated, CEINMS was executed with the model, muscle-tendon lengths, moment arms, and muscle activations as inputs, yielding L5-S1 joint moments as output.

2.3. Statistical analysis

Each repetition can be divided into five segments based on the lumbo-sacral flexion moment profile. For the analysis, the task was divided into two phases: the first consisting of lowering without weight and lifting with weight, and the second consisting of lowering with weight and lifting without weight (Figure 3). The approach of dividing the analysis between the two phases was chosen based on other literature papers that show differences between lifting the load and lowering it, in terms of biomechanics (Kim, 2010), risk to the spine (Larivière et al., 2002) and ergonomic reference indices (NIOSH).

The comparison of results was conducted from two perspectives: kinematics and dynamics. For the kinematic analysis, the L5-S1 flexion-extension angles derived from OMC and IMC were compared. For

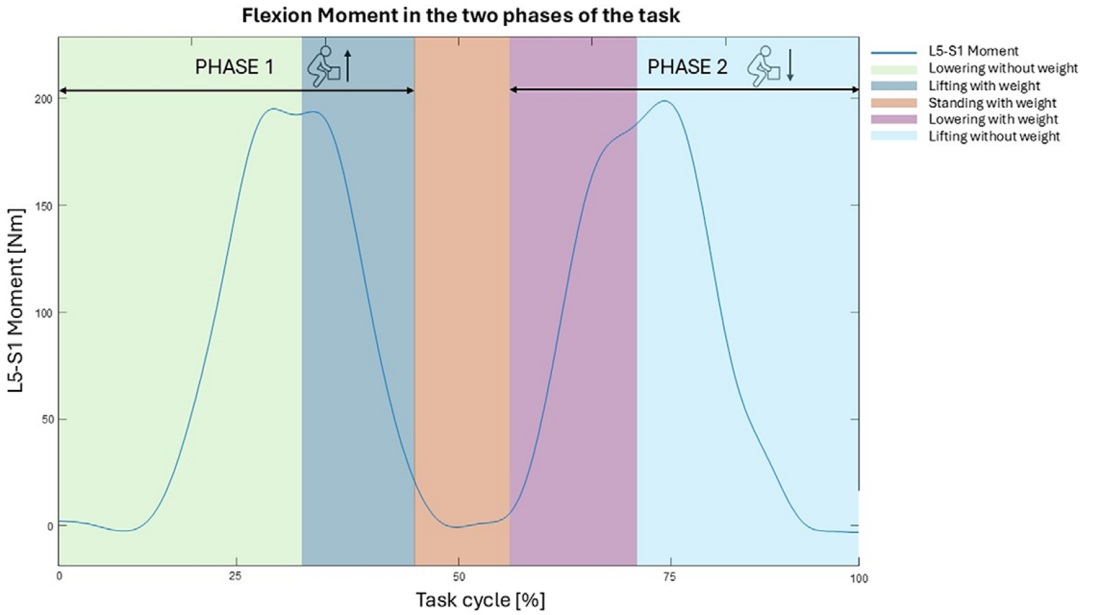


Figure 3. *Example of one trial of one subject of L5-S1 flexion moment division in the five segments and in the two phases of the task.*

Downloaded from https://www.cambridge.org/core. 19 Nov 2026 at 05:43:20, subject to the Cambridge Core terms of use.

the dynamic analysis, a three-way comparison was performed on the L5-S1 flexion moments obtained from three different methods: inverse dynamics (ID) using OMC data (gold standard), ID using IMC data, and CEINMS moments estimated after calibration with IMC data. After verifying the normality of the data, a multi-way ANOVA was conducted to assess the effects of subject, load, and their interaction. Since load was the only factor showing a significant effect, results were averaged across subjects.

3. Results

3.1. Lumbo-sacral flexion angle

Figure 4 depicts the average lumbo-sacral flexion angle over a cycle computed by OMC and IMC systems on all loads and types of lifting. An offset in the starting position is present, with the OMC already flexed at −2°.

In Figure 5, the average difference and its standard deviation of the maximum L5-S1 flexion angle are reported as a bar plot.

The mean difference between the two systems is 1.84° ± 0.86°. A one-sample *t*-test showed that this mean is significantly greater than zero ($t = 16.59$, $p < .001$), with a 95% confidence interval ranging from 1.62° to 2.06°. Looking at each load value, the discrepancies range from 1.1° to 2.4°, with slightly larger values observed at higher loads. The difference is always positive, meaning that the IMC underestimates the flexion angle. The variability, represented by the error bars, was limited and consistent across conditions, indicating stable performance of the IMC system in reproducing lumbar flexion angles.

3.2. Lumbo-sacral flexion moment

Table 1 reports the average and standard deviation values of the statistical parameters computed on the entire signals of the L5-S1 moment, comparing the OMC-based ID with IMC-based ID and CEINMS.

The direct comparison between L5-S1 flexion moment estimates obtained through inverse dynamics based on OMC and IMC data revealed a very high level of agreement between the two systems. Spearman correlation coefficients were consistently high across all lifting conditions (0.83–0.96). Reliability indices, including the ICC (ICC > 0.91) and the CMC (CMC ≈ 0.99), further confirmed the robustness of the dynamic reconstruction derived from the inertial sensors. The RMSE, averaging between 2.5 and 3 Nm, indicated good absolute precision with limited variation across loads, while the mean bias remained close to zero, suggesting the absence of systematic over- or underestimation trends. The comparison between OMC-based ID and CEINMS revealed very similar results between the two types of lifting: a strong correlation across all loading conditions, with Spearman coefficients ranging from 0.81 to 0.87. Reliability indices, including ICC (0.87–0.91) and CMC (>0.98), confirmed a high level of consistency and overall profile similarity. Mean bias remained low (0.14–2.22 Nm), suggesting the absence of substantial systematic errors; however, the widening confidence intervals at higher loads indicated increasing variability. Similarly, RMSE values rose from 5.52 to 9.75 Nm, accompanied by larger standard deviations, highlighting a reduction in absolute precision as the applied load increased.

Figure 6 depicts the average lumbo-sacral flexion moment over a cycle computed by ID from OMC and IMC data and computed by CEINMS on all loads and types of lifting. It should be noted that the higher L5-S1 flexion moments observed during squat compared to stoop refer to averaged data. A Mann–Whitney test performed between the max values of the moment between the two lifting techniques resulted in a lack of statistically significant difference. At the individual level, variability was present. The mean standard deviation of the average squat cycle for the OMC data varied from 0.3 Nm/kg at 5 kg of load to 0.7 Nm/kg at 0 kg, and for the stoop from 0.2 Nm/kg at 15 kg to 0.8 Nm/kg at 0 kg. These results highlight the high inter-subject variability and the relative magnitudes of the moments, which depend on each participant's lifting strategy, particularly the degree of trunk inclination and knee flexion adopted. It shows how there is an offset at the starting position and that the OMC moment is usually higher than the other two.

Downloaded from https://www.cambridge.org/core. 19 Nov 2026 at 05:43:20, subject to the Cambridge Core terms of use.

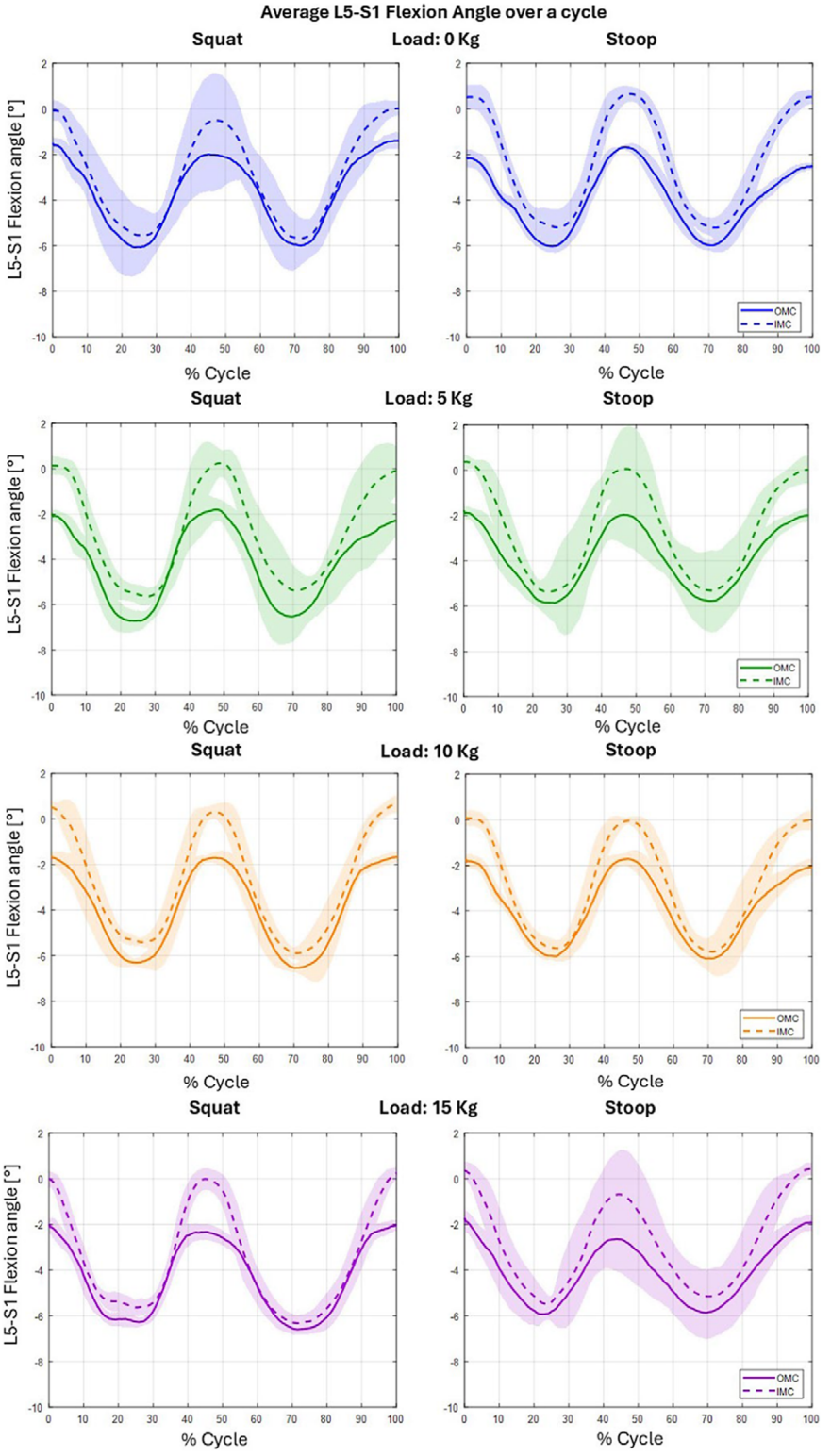


Figure 4. *Average and standard deviation of L5-S1 flexion angle over a cycle computed by OMC and IMC for each load and type of lifting.*

Downloaded from https://www.cambridge.org/core. 19 Nov 2026 at 05:43:20, subject to the Cambridge Core terms of use.

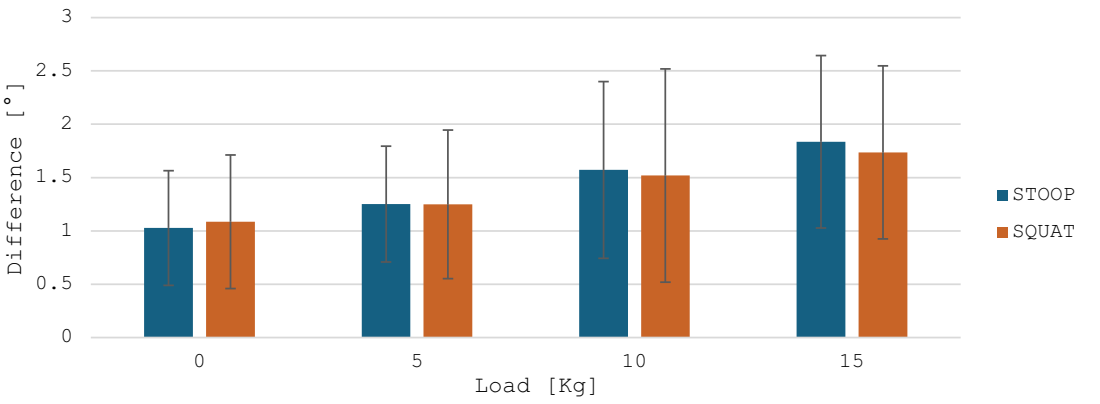


Figure 5. *Average and standard deviation of the difference of the maximum L5-S1 flexion angle between OMC and IMC for each load and type of lifting.*

Table 1. *Statistical parameters comparing the entire signal of lumbo-sacral flexion moment in the three methods*

Load			0 kg	5 kg	10 kg	15 kg
Spearman correlation coefficient (std) [−]	STOOP	OMC vs. IMC	0.94 (0.02)	0.90 (0.12)	0.94 (0.04)	0.91 (0.04)
		OMC vs. CEINMS	0.81 (0.07)	0.87 (0.05)	0.87 (0.04)	0.87 (0.10)
	SQUAT	OMC vs. IMC	0.83 (0.11)	0.95 (0.09)	0.96 (0.03)	0.93 (0.04)
		OMC vs. CEINMS	0.83 (0.08)	0.83 (0.08)	0.86 (0.03)	0.84 (0.04)
RMSE (std) [Nm]	STOOP	OMC vs. IMC	2.62 (1.00)	2.89 (1.96)	2.64 (2.91)	2.86 (0.46)
		OMC vs. CEINMS	5.52 (1.00)	7.95 (2.52)	8.03 (3.16)	9.75 (4.83)
	SQUAT	OMC vs. IMC	2.54 (0.82)	3.08 (1.96)	3.59 (2.27)	2.86 (1.90)
		OMC vs. CEINMS	5.61 (1.63)	6.08 (1.55)	5.81 (2.06)	6.75 (3.63)
Bland–Altman Bias (interval of confidence) [Nm]	STOOP	OMC vs. IMC	0.15 (11.45)	0.06 (15.39)	0.23 (21.65)	1.70 (28.34)
		OMC vs. CEINMS	1.98 (20.40)	1.32 (30.08)	0.64 (34.68)	0.72 (44.53)
	SQUAT	OMC vs. IMC	0.02 (14.61)	1.13 (20.79)	1.96 (30.78)	0.13 (34.84)
		OMC vs. CEINMS	1.01 (24.73)	2.00 (29.44)	2.22 (34.13)	0.14 (38.02)
Intraclass correlation (std) [−]	STOOP	OMC vs. IMC	0.98 (0.00)	0.97 (0.02)	0.97 (0.02)	0.95 (0.05)
		OMC vs. CEINMS	0.91 (0.04)	0.90 (0.06)	0.90 (0.06)	0.87 (0.07)
	SQUAT	OMC vs. IMC	0.96 (0.04)	0.96 (0.09)	0.92 (0.01)	0.91 (0.07)
		OMC vs. CEINMS	0.89 (0.06)	0.90 (0.03)	0.89 (0.03)	0.89 (0.87)
Coefficient of multiple correlation (std) [−]	STOOP	OMC vs. IMC	0.99 (0.00)	0.99 (0.00)	0.99 (0.00)	0.99 (0.00)
		OMC vs. CEINMS	0.98 (0.00)	0.98 (0.00)	0.98 (0.00)	0.98 (0.00)
	SQUAT	OMC vs. IMC	0.98 (0.00)	0.99 (0.00)	0.99 (0.00)	0.99 (0.00)
		OMC vs. CEINMS	0.98 (0.00)	0.98 (0.00)	0.98 (0.00)	0.98 (0.01)

Note: The values are the average and standard deviation of the results for each load value, except for the Bland–Altman Bias and interval of confidence.

Table 2 reports the values of the average difference between the average maximum and mean values of lumbo-sacral moments in a cycle from OMC-based ID with respect to IMC-based ID and CEINMS.

During Phase 1, the maximum moment was almost consistently underestimated by IMC-based ID and CEINMS, as shown by the low number of green cells, with increasing discrepancies at higher loads, especially for CEINMS in squat (from −4.30 Nm at 0 kg to −20.79 Nm at 15 kg). Conversely, during Phase 2, while IMC-based presented a similar trend in Phase 1, differences in maximum moment were smaller for CEINMS in squat (ranging between −0.46 and + 1.88 Nm) and stoop for 0 to 10 kg (−5.57 to 2.52 Nm), with a higher difference only in stoop at 15 kg.

Mean moment analysis revealed heterogeneous outcomes for CEINMS: while differences during Phase 2 remained limited (−3.69 to +5.43 Nm), Phase 1, and especially squat, showed larger discrepancies, particularly at 15 kg (+9.93 Nm in stoop and +17.83 Nm for squat). IMC-based ID instead presents stable, low error across all loads and types of lifting.

Downloaded from https://www.cambridge.org/core. 19 Nov 2026 at 05:43:20, subject to the Cambridge Core terms of use.

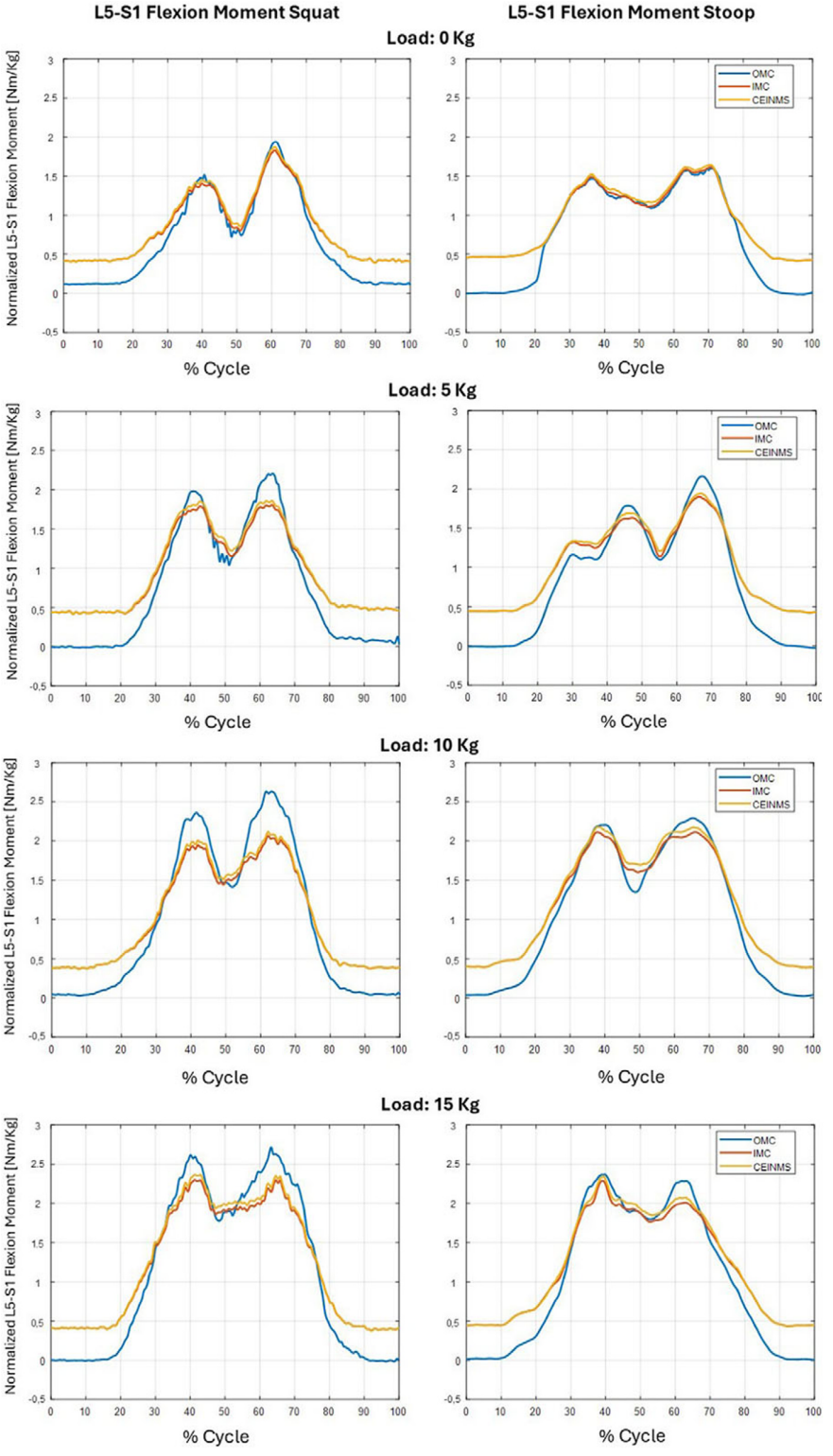


Figure 6. *Average L5-S1 flexion moment over a cycle computed by OMC, IMC, and CEINMS for each load and type of lifting.*

Downloaded from https://www.cambridge.org/core. 19 Nov 2026 at 05:43:20, subject to the Cambridge Core terms of use.

Table 2. *Values of the average (and standard deviation) difference between the maximum and mean values of moment over a cycle by the IMC-based ID and CEINMS compared to OMC-based ID methods during lifting and lowering*

Load			0 kg	5 kg	10 kg	15 kg
Difference in max moment during Phase 1 (std) [Nm]	STOOP	OMC vs. IMC	−5.61 (1.21)	−14.78 (9.50)	−13.58 (7.32)*	−8.58 (6.16)
		OMC vs. CEINMS	−8.25 (5.24)*	−13.36 (6.91)*	−14.27 (4.51)*	−14.44 (12.32)
	SQUAT	OMC vs. IMC	−3.28 (1.19)	−7.60 (2.21)	−7.19 (1.36)	−12.61 (12.19)
		OMC vs. CEINMS	−4.30 (5.55)	−15.58 (2.71)*	−18.15 (12.13)*	−20.79 (11.75)*
Difference in max moment during Phase 2 (std) [Nm]	STOOP	OMC vs. IMC	−4.67 (1.76)	−10.86 (1.74)*	−13.76 (8.56)	−3.48 (9.24)
		OMC vs. CEINMS	2.52 (1.84)	−3.62 (1.90)	−5.57 (4.50)	−16.59 (9.65)
	SQUAT	OMC vs. IMC	−3.62 (1.63)	−4.12 (0.10)	−8.72 (0.41)	−12.36 (8.65)*
		OMC vs. CEINMS	−0.12 (1.75)	0.55 (2.80)	1.88 (4.05)	−0.46 (6.10)
Difference in mean moment during Phase 1 (std) [Nm]	STOOP	OMC vs. IMC	−1.08 (0.47)	−0.64 (2.35)	−0.72 (5.04)	−0.57 (0.98)
		OMC vs. CEINMS	0.08 (0.07)	3.52 (1.20)	6.48 (1.98)*	9.93 (6.11)
	SQUAT	OMC vs. IMC	−0.31 (1.16)	−3.09 (1.06)	−7.19 (0.36)	−1.70 (18.25)
		OMC vs. CEINMS	3.88 (0.90)	1.57 (0.60)	11.90 (9.45)*	17.83 (8.05)*
Difference in mean moment during Phase 2 (std) [Nm]	STOOP	OMC vs. IMC	0.32 (1.82)	2.81 (0.85)	1.89 (5.40)	−3.48 (9.24)
		OMC vs. CEINMS	−1.68 (0.05)	2.79 (0.9)	1.06 (0.08)	5.43 (4.35)
	SQUAT	OMC vs. IMC	−0.78 (1.43)	−1.94 (1.00)	−0.54 (0.65)	−2.63 (1.65)
		OMC vs. CEINMS	−1.90 (0.80)*	−3.69 (0.80)*	0.50 (0.03)	−4.44 (4.67)

Note: The positive differences, indicating an overestimation, are highlighted in green. The statistically significant differences are reported with an asterisk.

Figure 7 shows the average maximum (left) and mean (right) L5-S1 flexion moments normalized over the body weight obtained with the OMC-based ID and CEINMS during the two phases of the stoop and squat task at different loads.

In all cases, flexion moments increased progressively with the external load, as expected. For the maximum values, CEINMS tended to slightly underestimate the moments compared to OMC during lifting, particularly at 10 and 15 kg, whereas differences were smaller and more consistent during lowering. Regarding mean moments, the two systems exhibited closer agreement across all loads, with only minor discrepancies observed at higher loads during lifting. Overall, both systems captured the

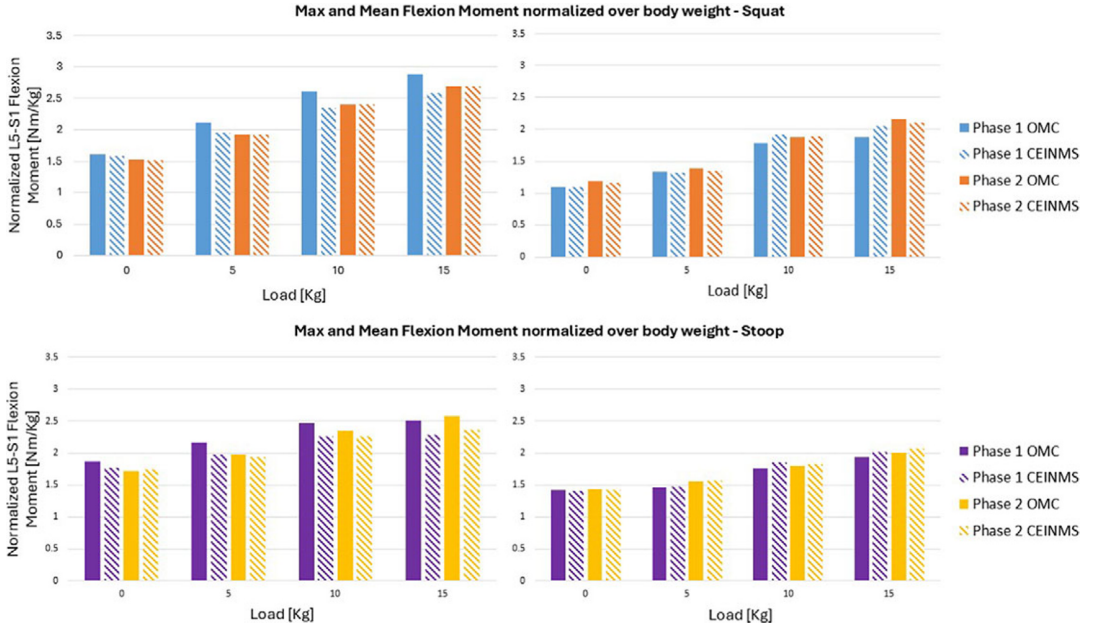


Figure 7. *Average maximum (left) and mean (right) values of lumbo-sacral moment for the two types of lifting in the two phases from OMC-based ID and CEINMS for each load.*

Downloaded from https://www.cambridge.org/core. 19 Nov 2026 at 05:43:20, subject to the Cambridge Core terms of use.

load-dependent increase in lumbar moments, with the largest deviations occurring for peak values in the lifting phase, while mean values and lowering phases showed higher consistency between methods.

4. Discussion and conclusion

This study shows that the CEINMS framework, combined with IMC and sEMG signals, can provide a robust alternative to gold-standard laboratory approaches for estimating lumbar joint moments. These findings are in line with previous studies reporting root mean square (RMS) errors around 20 Nm and high ICCs in IMU-based estimation of spinal kinetics during trunk bending and manual handling tasks (Faber et al., 2016; Matijevich et al., 2021). The present results extend this evidence to symmetric lifting tasks, reinforcing the potential of wearables for ecological assessments outside laboratory environments.

Inverse kinematics and inverse dynamics were performed using OpenSim (Delp et al., 2007; Seth et al., 2018), a widely adopted and validated framework for musculoskeletal modeling. The use of OpenSim ensured methodological consistency with the musculoskeletal model and facilitated integration with the CEINMS framework (Pizzolato et al., 2015). Importantly, the LFB model employed in this study was specifically developed and validated for lifting tasks within the OpenSim environment (Beaucage-Gauvreau et al., 2019), providing explicit support for the estimation of lumbar spine loads at the L5-S1 joint during symmetric lifting, which directly aligns with the scope of this work. The LFB model includes detailed trunk musculature and lumbar vertebral degrees of freedom, making it particularly suited for the analysis of spinal loading during manual material handling (Beaucage-Gauvreau et al., 2019; Manoharan et al., 2023).

Regarding the muscle force estimation framework, it is worth noting that CEINMS is not the sole option for performing EMG-informed neuromusculoskeletal modelling as presented in the introduction chapter. However, CEINMS offers distinct advantages that motivated its adoption in this study: it operates on dynamic skeletal models with any number of degrees of freedom and MTUs, supports multiple neural control solutions (EMG-driven, EMG-assisted, and static optimization) within the same framework, enables subject-specific calibration of neuromuscular parameters, and integrates with OpenSim (Pizzolato et al., 2015). Studies applying a similar pipeline have demonstrated its effectiveness across a range of dynamic tasks, including walking (Bu et al., 2023), cycling (Crossley et al., 2025), and high-speed locomotion (Akhundov et al., 2022), confirming its suitability for tasks involving complex multi-joint coordination. A custom IK/ID pipeline could potentially allow greater control over joint definitions and model assumptions; however, replicating the validated procedures embedded in OpenSim was beyond the scope of this work, and any systematic offset introduced by the standardized pipeline would be consistent across tasks and participants, making it a reproducible and comparable source of variability rather than a task-specific confound.

In addition to the CEINMS validation, the comparison between IMC- and OMC-based ID revealed an excellent level of agreement, as reported in Table 1, confirming the reliability of the IMC system in reproducing lumbar joint kinetics. The strong correlations (ρ = 0.83–0.96) and high reliability indices (ICC > 0.91, CMC ≈ 0.99) indicate that IMC-based estimates can accurately replicate the temporal evolution and magnitude of the L5-S1 flexion moments observed with OMC. The low RMSE (≈2.5–3 Nm) and near-zero bias further suggest that the differences between the two systems are minimal, supporting the feasibility of IMC for standalone use in dynamic lifting analysis. Looking at the moment average graphs (Figure 6), the initial offset in starting values could be due to the offset present at the initial state in the flexion angle, as reported in Figure 4.

A key observation concerns the underestimation of peak flexion moments during the lifting phase, which became more pronounced with heavier loads, as reported in Table 2 and Figure 7 and in accordance with Muller et al. (2022). This is probably due to the increasing difference in flexion angle as reported in Figure 5 rather than to the recorded muscle activation. In OS, individual intervertebral joint angles are not directly measured. Instead, the model estimates the L5-S1 angle and assumes proportional motion across the other lumbar levels. Therefore, discrepancies between OMC and IMC-based estimates likely arise from differences in segment orientation estimation.

Downloaded from https://www.cambridge.org/core. 19 Nov 2026 at 05:43:20, subject to the Cambridge Core terms of use.

Several factors may contribute to the observed underestimation. First, IMU sensor-fusion and filtering algorithms tend to smooth extreme joint excursions (Morrow et al., 2017; Dal Farra et al., 2025). Second, small misalignments between sensors and anatomical segments, combined with calibration constraints, can introduce angular biases that propagate non-linearly into joint moment estimation, especially under high external loads (Shakourisalim et al., 2024). Third, soft-tissue artefacts and frame-definition differences can also affect OMC outputs in distinct ways compared with IMC. Increasing sensor density along the lumbar region could enhance the resolution of multi-segmental motion and mitigate some of these error sources (Moon et al., 2022; Beange et al., 2024).

From an application standpoint, the relatively low bias and high agreement of CEINMS (calibrated from IMC data) across loads highlight the promise of IMUs and sEMG-driven models for ergonomic risk assessment and workplace monitoring. Even if peak loads are slightly underestimated, the wearable approach successfully captured the expected load-dependent increase in lumbar moments, which is the key feature for evaluating relative changes in mechanical exposure across tasks or conditions. This suggests that wearable-driven estimates may be sufficient to identify hazardous lifting scenarios and support preventive interventions in occupational settings.

Interestingly, group-averaged results (Figure 6) showed slightly higher L5-S1 flexion moments during squat compared to stoop, even for the gold-standard OMC. Meaning that these results are not related to CEINMS or even IMC but are a direct cause of the kinematics strategies of the subjects, as reported also in the literature (Van Dieën et al., 1999; Bazrgari et al., 2007; Van Der Have et al., 2019). This may appear counterintuitive, as stoop lifting is often associated with a larger trunk moment arm relative to L5-S1, the effective joint moment depends not only on trunk inclination but also on the overall lifting strategy, including knee flexion, hip contribution, and vertical displacement of the load. Inter-subject variability was observed, and the relative magnitude of squat versus stoop moments was influenced by the actual trunk and knee kinematics adopted. Starting from the L5-S1 flexion angle, which, as reported in Figure 4, showed slightly larger values in squat rather than stoop. This is a direct cause of the increasing moment values. Therefore, these findings should not be interpreted as a general biomechanical rule but rather as task- and strategy-dependent outcomes.

Some limitations should be acknowledged. First, the sample size was small and limited to young, healthy adults, which restricts generalizability to workers of different ages, body compositions, or individuals with musculoskeletal conditions. Second, calibration was performed only at 0 and 15 kg to evaluate the ability of the model to generalize across intermediate loads. An alternative approach would have been to calibrate across all loading conditions to maximize accuracy. However, this would have reduced the possibility of testing its generalization performance. Future studies could compare these calibration strategies to evaluate the trade-off between accuracy and generalizability. Lastly, from an application standpoint, it is important to note that sensor placement accuracy remains a crucial aspect. However, the procedure is straightforward and can be easily learned after minimal training, making it feasible for use in workplace settings. Standardized positioning protocols and quick calibration routines could further enhance repeatability and reduce operator dependency, supporting consistent measurements across different users and environments.

Since the difference in terms of L5-S1 flexion angle ROM is not negligible, future research should focus on improving the accuracy of the IK computed from IMU for such small joints. Moreover, a larger and more diverse population should be explored, including real-world lifting scenarios with variable asymmetry and dynamics, and investigating the integration of multi-sensor lumbar configurations. Moreover, coupling wearable-based kinetic estimates with fatigue or discomfort measures could broaden the applicability of such systems in occupational health.

In conclusion, this study provides strong validation evidence for a wearable-only approach to estimating L5-S1 flexion-extension moments. While peak values during lifting under heavy loads are underestimated, the overall accuracy and reliability are high, supporting the feasibility of using IMUs and sEMG-based neuromusculoskeletal models for field applications in ergonomics and occupational biomechanics.

Abbreviations

CEINMS	calibrated EMG-informed neuromusculoskeletal
FE	finite element
IMC	inertial motion capture

Downloaded from https://www.cambridge.org/core. 19 Nov 2026 at 05:43:20, subject to the Cambridge Core terms of use.

OMC	optoelectronic motion capture system
OS	OpenSim

Data availability statement. Data can be made available to interested researchers upon request by email to the corresponding author.

Authorship contribution. M.S., M.I.R., and F.M. designed the study; F.M. conducted data acquisition and formal analysis; M.S. and M.I.R. supervised data collection and processing; M.S., M.I.R., and F.M. wrote the article; and T.V., M.G., and A.R. revised the manuscript. M.S. and M.G. equally supervised the work.

Funding statement. This work was partly funded by the ERC Consolidator Grant ROBOREACTOR (Grant No. 101123866), the Netherlands Sectorplan Techniek II, and the EU RIA project SWAG (Grant No. 101120408). Open access funding provided by University of Twente.

Competing interests. The authors declare no competing interests exist.

Ethical standards. The authors assert that all procedures contributing to this work comply with the ethical standards of the relevant national and institutional committees on human experimentation and with the Helsinki Declaration of 1975, as revised in 2008.

AI tools use. The authors declare that AI tool (ChatGPT5a) was used on November 10, 2025, only for grammar checks and rephrasing of some sentences, but not for producing completely new text.

References

Abdullah M, **Hulleck AA**, **Katmah R**, **Khalaf K and El-Rich M** (2024) Multibody dynamics-based musculoskeletal modeling for gait analysis: A systematic review. *Journal of Neuroengineering and Rehabilitation* **21**(1), 178. https://doi.org/10.1186/s12984-024-01458-y.

Akhundov R, **Saxby DJ**, **Diamond LE**, **Edwards S**, **Clausen P**, **Dooley K**, **Blyton S and Snodgrass SJ** (2022) Is subject-specific musculoskeletal modelling worth the extra effort or is generic modelling worth the shortcut? *PLoS One* **17**(1), e0262936. https://doi.org/10.1371/journal.pone.0262936.

Al Borno M, **O'Day J**, **Ibarra V**, **Dunne J**, **Seth A**, **Habib A**, **Ong C**, **Hicks J**, **Uhlrich S and Delp S** (2022) OpenSense: An open-source toolbox for inertial-measurement-unit-based measurement of lower extremity kinematics over long durations. *Journal of Neuroengineering and Rehabilitation* **19**(1), 22. https://doi.org/10.1186/s12984-022-01001-x.

Bazrgari B, **Shirazi-Adl A and Arjmand N** (2007) Analysis of squat and stoop dynamic liftings: Muscle forces and internal spinal loads. *European Spine Journal* **16**(5), 687–699. https://doi.org/10.1007/s00586-006-0240-7.

Beange KHE, **Chan ADC and Graham RB** (2024) Investigating concurrent validity of inertial sensors to evaluate multiplanar spine movement. *Journal of Biomechanics* **164**, 111939. https://doi.org/10.1016/j.jbiomech.2024.111939.

Beaucage-Gauvreau E, **Robertson WSP**, **Brandon SCE**, **Fraser R**, **Freeman BJC**, **Graham RB**, **Thewlis D and Jones CF** (2019) Validation of an OpenSim full-body model with detailed lumbar spine for estimating lower lumbar spine loads during symmetric and asymmetric lifting tasks. *Computer Methods in Biomechanics and Biomedical Engineering* **22**(5), 451–464. https://doi.org/10.1080/10255842.2018.1564819.

Bu A, **MacLean MK and Ferris DP** (2023) EMG-informed neuromuscular model assesses the effects of varied bodyweight support on muscles during overground walking. *Journal of Biomechanics* **151**, 111532. https://doi.org/10.1016/j.jbiomech.2023.111532.

Buchanan TS, **Lloyd DG**, **Manal K and Besier TF** (2004) Neuromusculoskeletal modeling: Estimation of muscle forces and joint moments and movements from measurements of neural command. *Journal of Applied Biomechanics* **20**(4), 367–395. https://doi.org/10.1123/jab.20.4.367.

Coenen P, **Gouttebarge V**, **Van Der Burght ASAM**, **Van Dieën JH**, **Frings-Dresen MHW**, **Van Der Beek AJ and Burdorf A** (2014) The effect of lifting during work on low back pain: A health impact assessment based on a meta-analysis. *Occupational and Environmental Medicine* **71**(12), 871–877. https://doi.org/10.1136/oemed-2014-102346.

Coenen P, **Kingma I**, **Boot CRL**, **Twisk JWR**, **Bongers PM and Van Dieën JH** (2013) Cumulative low back load at work as a risk factor of low back pain: A prospective cohort study. *Journal of Occupational Rehabilitation* **23**(1), 11–18. https://doi.org/10.1007/s10926-012-9375-z.

Crossley CB, **Worsey MTO**, **Diamond LE**, **Saxby DJ**, **Wackwitz T**, **Bourne MN**, **Lloyd DG and Pizzolato C** (2025) A calibrated EMG-informed neuromusculoskeletal model can estimate hip and knee joint contact forces in cycling better than static optimisation. *Journal of Biomechanics* **182**, 112586. https://doi.org/10.1016/j.jbiomech.2025.112586.

Crowninshield RD and Brand RA (1981) A physiologically based criterion of muscle force prediction in locomotion. *Journal of Biomechanics* **14**(11), 793–801. https://doi.org/10.1016/0021-9290(81)90035-X.

Dal Farra F, **Cerfoglio S**, **Porta M**, **Pau M**, **Galli M**, **Lopomo NF and Cimolin V** (2025) Comparative assessment of an IMU-based wearable device and a marker-based optoelectronic system in trunk motion analysis: A cross-sectional investigation. *Applied Sciences* **15**(11), 5931. https://doi.org/10.3390/app15115931.

Downloaded from https://www.cambridge.org/core. 19 Nov 2026 at 05:43:20, subject to the Cambridge Core terms of use.

Delp SL, **Anderson FC**, **Arnold AS**, **Loan P**, **Habib A**, **John CT**, **Guendelman E and Thelen DG** (2007) OpenSim: Open-source software to create and analyze dynamic simulations of movement. *IEEE Transactions on Biomedical Engineering* **54**(11), 1940–1950. https://doi.org/10.1109/TBME.2007.901024.

Elliott G, **Sawicki GS**, **Marecki A and Herr H** (2013) The biomechanics and energetics of human running using an elastic knee exoskeleton. In *2013 IEEE 13th International Conference on Rehabilitation Robotics (ICORR)*, pp. 1–6. https://doi.org/10.1109/ICORR.2013.6650418

Faber GS, **Chang CC**, **Kingma I**, **Dennerlein JT and Van Dieën JH** (2016) Estimating 3D L5/S1 moments and ground reaction forces during trunk bending using a full-body ambulatory inertial motion capture system. *Journal of Biomechanics* **49**(6), 904–912. https://doi.org/10.1016/j.jbiomech.2015.11.042.

Feola E, **Refai MIM**, **Costanzi D**, **Sartori M and Calanca A** (2023) A neuromechanical model-based strategy to estimate the operator's payload in industrial lifting tasks. *IEEE Transactions on Neural Systems and Rehabilitation Engineering* **31**, 4644–4652. https://doi.org/10.1109/TNSRE.2023.3334993.

Galbusera F, **Cina A**, **Panico M**, **Albano D and Messina C** (2020) Image-based biomechanical models of the musculoskeletal system. *European Radiology Experimental* **4**(1), 49. https://doi.org/10.1186/s41747-020-00172-3.

Geisser ME, **Ranavaya M**, **Haig AJ**, **Roth RS**, **Zucker R**, **Ambroz C and Caruso M** (2005) A meta-analytic review of surface electromyography among persons with low back pain and normal, healthy controls. *The Journal of Pain* **6**(11), 711–726. https://doi.org/10.1016/j.jpain.2005.06.008.

Ghamkhar L and Kahlaee AH (2015) Trunk muscles activation pattern during walking in subjects with and without chronic low back pain: A systematic review. *PM&R* **7**(5), 519–526. https://doi.org/10.1016/j.pmrj.2015.01.013

Jahn A, **Andersen JH**, **Christiansen DH**, **Seidler A and Dalbøge A** (2023) Occupational mechanical exposures as risk factor for chronic low-back pain: A systematic review and meta-analysis. *Scandinavian Journal of Work, Environment & Health* **49**(7), 453–465. https://doi.org/10.5271/sjweh.4114.

Kim HK (2010) Comparison of lifting and lowering activity based on biomechanical, physiological, psychophysical criteria. *Journal of the Ergonomics Society of Korea* **29**(1), 145–153. https://doi.org/10.5143/JESK.2010.29.1.145.

Larivière C, **Gagnon D and Loisel P** (2002) A biomechanical comparison of lifting techniques between subjects with and without chronic low back pain during freestyle lifting and lowering tasks. *Clinical Biomechanics* **17**(2), 89–98. https://doi.org/10.1016/S0268-0033(01)00106-1.

Lathlean TJH, **Ramachandran AK**, **Sim S and Whittle IR** (2024) The clinical utility and reliability of surface electromyography in individuals with chronic low back pain: A systematic review. *Journal of Clinical Neuroscience* **129**, 110877. https://doi.org/10.1016/j.jocn.2024.110877.

Li J, **Lu Y**, **Miller SC**, **Jin Z and Hua X** (2019) Development of a finite element musculoskeletal model with the ability to predict contractions of three-dimensional muscles. *Journal of Biomechanics* **94**, 230–234. https://doi.org/10.1016/j.jbiomech.2019.07.042.

Lloyd DG and Besier TF (2003) An EMG-driven musculoskeletal model to estimate muscle forces and knee joint moments in vivo. *Journal of Biomechanics* **36**(6), 765–776. https://doi.org/10.1016/S0021-9290(03)00010-1

Manoharan P, **Pranata A**, **Tse KM and Chai R** (2023) Estimation of lumbar spine loading of low back pain participant during lifting using an open source musculoskeletal model. In *2023 45th Annual International Conference of the IEEE Engineering in Medicine & Biology Society (EMBC)*, pp. 1–4. https://doi.org/10.1109/EMBC40787.2023.10340362

Matijevich ES, **Volgyesi P and Zelik KE** (2021) A promising wearable solution for the practical and accurate monitoring of low back loading in manual material handling. *Sensors* **21**(2), 340. https://doi.org/10.3390/s21020340.

Mohamed Refai MI, **Moya-Esteban A and Sartori M** (2024) Electromyography-driven musculoskeletal models with time-varying fatigue dynamics improve lumbosacral joint moments during lifting. *Journal of Biomechanics* **164**, 111987. https://doi.org/10.1016/j.jbiomech.2024.111987.

Moon KS, **Gombatto SP**, **Phan K and Ozturk Y** (2022) Extraction of lumbar spine motion using a 3-IMU wearable cluster. *Sensors* **23**(1), 182. https://doi.org/10.3390/s23010182.

Morrow MMB, **Lowndes B**, **Fortune E**, **Kaufman KR and Hallbeck MS** (2017) Validation of inertial measurement units for upper body kinematics. *Journal of Applied Biomechanics* **33**(3), 227–232. https://doi.org/10.1123/jab.2016-0120.

Motta F, **Chieffo C**, **Monoli C**, **Tuhtan JA and Galli M** (2025) Land and underwater estimation of joint angles using MOCAP, experimental IMUs, and OpenSense. *IEEE Sensors Journal* **25**(12), 21275–21283. https://doi.org/10.1109/JSEN.2025.3565835.

Motta F, **Varrecchia T**, **Chini G**, **Ranavolo A and Galli M** (2024) The use of wearable systems for assessing work-related risks related to the musculoskeletal system—A systematic review. *International Journal of Environmental Research and Public Health* **21**(12), 1567. https://doi.org/10.3390/ijerph21121567.

Moya-Esteban A, **Van Der Kooij H and Sartori M** (2022) Robust estimation of lumbar joint forces in symmetric and asymmetric lifting tasks via large-scale electromyography-driven musculoskeletal models. *Journal of Biomechanics* **144**, 111307. https://doi.org/10.1016/j.jbiomech.2022.111307.

Muller A, **Mecheri H**, **Corbeil P**, **Plamondon A and Robert-Lachaine X** (2022) Inertial motion capture-based estimation of L5/S1 moments during manual materials handling. *Sensors* **22**(17), 6454. https://doi.org/10.3390/s22176454.

Murtezani A, **Ibraimi Z**, **Sllamniku S**, **Osmani T and Sherifi S** (2011). Prevalence and risk factors for low back pain in industrial workers. *Folia Medica* **53**(3). https://doi.org/10.2478/v10153-011-0060-3.

Downloaded from https://www.cambridge.org/core. 19 Nov 2026 at 05:43:20, subject to the Cambridge Core terms of use.

Nail-Ulloa I, **Huangfu R**, **Zabala M**, **Bani Hani D**, **Pool N**, **Chen H**, **Schall MC**, **Sesek R and Gallagher S** (2024) Assessing the accuracy of a wireless sensor system for estimating lumbar moments during manual lifting tasks considering the effects of load weight, asymmetry, and height. *International Journal of Industrial Ergonomics* **103**, 103636. https://doi.org/10.1016/j.ergon.2024.103636.

Palmieri M, **Donno L**, **Cimolin V and Galli M** (2023) Cervical range of motion assessment through inertial technology: A validity and reliability study. *Sensors* **23**(13), 6013. https://doi.org/10.3390/s23136013.

Papi E, **Koh WS and McGregor AH** (2017) Wearable technology for spine movement assessment: A systematic review. *Journal of Biomechanics* **64**, 186–197. https://doi.org/10.1016/j.jbiomech.2017.09.037.

Pizzolato C, **Lloyd DG**, **Sartori M**, **Ceseracciu E**, **Besier TF**, **Fregly BJ and Reggiani M** (2015) CEINMS: A toolbox to investigate the influence of different neural control solutions on the prediction of muscle excitation and joint moments during dynamic motor tasks. *Journal of Biomechanics* **48**(14), 3929–3936. https://doi.org/10.1016/j.jbiomech.2015.09.021.

Roetenberg D, **Luinge H and Slycke P** (2009) *Xsens MVN: Full 6DOF Human Motion Tracking Using Miniature Inertial Sensors*.

Rook JWA, **Sartori M and Refai MI** (2025) Toward wearable electromyography for personalized musculoskeletal trunk models using an inverse synergy-based approach. *IEEE Transactions on Medical Robotics and Bionics* **7**(1), 13–19. https://doi.org/10.1109/TMRB.2024.3503900.

Seth A, **Hicks JL**, **Uchida TK**, **Habib A**, **Dembia CL**, **Dunne JJ**, **Ong CF**, **DeMers MS**, **Rajagopal A**, **Millard M**, **Hamner SR**, **Arnold EM**, **Yong JR**, **Lakshmikanth SK**, **Sherman MA**, **Ku JP and Delp SL** (2018) OpenSim: Simulating musculoskeletal dynamics and neuromuscular control to study human and animal movement. *PLoS Computational Biology* **14**(7), e1006223. https://doi.org/10.1371/journal.pcbi.1006223.

Shakourisalim M, **Martinez KB**, **Golabchi A**, **Tavakoli M and Rouhani H** (2024) Estimation of lower back muscle force in a lifting task using wearable IMUs. *Journal of Biomechanics* **167**, 112077. https://doi.org/10.1016/j.jbiomech.2024.112077.

Van Der Have A, **Van Rossom S and Jonkers I** (2019) Squat lifting imposes higher peak joint and muscle loading compared to stoop lifting. *Applied Sciences* **9**(18), 3794. https://doi.org/10.3390/app9183794.

Van Dieën JH, **Hoozemans MJM and Toussaint HM** (1999) Stoop or squat: A review of biomechanical studies on lifting technique. *Clinical Biomechanics* **14**(10), 685–696. https://doi.org/10.1016/S0268-0033(99)00031-5.

Varrecchia T, **Conforto S**, **De Nunzio AM**, **Draicchio F**, **Falla D and Ranavolo A** (2022) Trunk muscle coactivation in people with and without low back pain during fatiguing frequency-dependent lifting activities. *Sensors* **22**(4), 1417. https://doi.org/10.3390/s22041417.

Varrecchia T, **Motta F**, **Chini G**, **Galli M and Ranavolo A** (2024) Enhanced biomechanical risk assessment in manual lifting: Comparing inertial measurement units with optoelectronic systems for composite lifting index calculation. *Applied Sciences* **14**(23), 11292. https://doi.org/10.3390/app142311292.

Vera-Garcia FJ, **Moreside JM and McGill SM** (2010) MVC techniques to normalize trunk muscle EMG in healthy women. *Journal of Electromyography and Kinesiology* **20**(1), 10–16. https://doi.org/10.1016/j.jelekin.2009.03.010.

Villa G, **Cerfoglio S**, **Bonfiglio A**, **Capodaglio P**, **Galli M and Cimolin V** (2025) Validation of a commercially available IMU-based system against an optoelectronic system for full-body motor tasks. *Sensors* **25**(12), 3736. https://doi.org/10.3390/s25123736.

Cite this article: Motta F, Refai MI, Ranavolo A, Varrecchia T, Sartori M and Galli M (2026) Wearable-only estimation of L5-S1 joint moments during lifting: A CEINMS-based validation. *Wearable Technologies*, 7, e12. doi:https://doi.org/10.1017/wtc.2026.10047

Downloaded from https://www.cambridge.org/core. 19 Nov 2026 at 05:43:20, subject to the Cambridge Core terms of use.